Received: 3 October 2022 | Revised: 4 May 2023 | Accepted: 10 May 2023

DOI: 10.1111/psyp.14360

PSYCHOPHYSIOLOGY SPR WILEY

ORIGINAL ARTICLE

Early development of electrophysiological activity: Contribution of periodic and aperiodic components of the EEG signal

Josué Rico-Picó[1,2] | Sebastián Moyano[1,2] | Ángela Conejero[1,3] | Ángela Hoyo[2] | M. Ángeles Ballesteros-Duperón[1,4] | M. Rosario Rueda[1,2]

[1]Mind, Brain and Behavior Research Center (CIMCYC), University of Granada, Granada, Spain

[2]Department of Experimental Psychology, University of Granada, Granada, Spain

[3]Department of Developmental and Educational Psychology, University of Granada, Granada, Spain

[4]Department of Psychobiology, University of Granada, Granada, Spain

Correspondence
M. Rosario Rueda, Mind, Brain and Behavior Research Center (CIMCYC), University of Granada, Campus de Cartuja, S/N, 18071 Granada, Spain.
Email: rorueda@ugr.es

Funding information
Fundación Tatiana Pérez de Guzmán el Bueno, Grant/Award Number: Predoctoral Fellowship in Neuroscience (2019); National Research Agency of Spain, Grant/Award Number: PID2020-113996GB-I00 and PSI2017-82670-P

Abstract

Brain function rapidly changes in the first 2 years of life. In the last decades, resting-state EEG has been widely used to explore those changes. Previous studies have focused on the relative power of the signal in established frequency bands (i.e., theta, alpha, and beta). However, EEG power is a mixture of a 1/f-like background power (aperiodic) in combination with narrow peaks that appear over that curve (periodic activity, e.g., alpha peak). Therefore, it is possible that relative power captures both, aperiodic and periodic brain activity, contributing to changes in electrophysiological activity observed in infancy. For this reason, we explored the early developmental trajectory of the relative power in theta, alpha, and beta frequency bands from infancy to toddlerhood and compared it with changes in periodic activity in a longitudinal study with three waves at age 6, 9, and 16 to 18 months. Finally, we tested the contribution of periodic activity and aperiodic components of the EEG to age changes in relative power. We found that relative power and periodic activity trajectories differed in this period in all the frequency bands but alpha. Furthermore, aperiodic EEG activity flattened between 6 and 18 months. More importantly, only alpha relative power was exclusively related to periodic activity, whereas aperiodic components of the signal significantly contributed to the relative power of activity in theta and beta bands. Thus, relative power in these frequencies is influenced by developmental changes of the aperiodic activity, which should be considered for future studies.

KEYWORDS

alpha, aperiodic EEG activity, beta, development, infancy, periodic EEG activity, resting EEG, theta, toddlerhood

1 | INTRODUCTION

Profound changes in the structure of the brain and its function take place in the first years of life, which has been related to the emergence and development of diverse cognitive processes (Gabard-Durnam & McLaughlin, 2020; Gilmore et al., 2018). Among all the techniques that measure brain function, electroencephalography (EEG) has been widely used to characterize functional development in infants and toddlers due to the easiness and adaptability of its application (Saby & Marshall, 2012).

The EEG signal offers information about neural oscillations, reflecting the synchronization and desynchronization of neuronal activation at different rhythms in both micro and macro neural circuits (Buzsáki, 2006; Buzsáki & Draguhn, 2004; Cohen, 2017; see Buzsáki et al., 2012 for a review). Baseline EEG activity is usually recorded at rest (resting-state EEG; rs-EEG), offering information about the intrinsic activity of the brain without the constraints of a task. As a result, the rs-EEG has been widely implemented to explore brain function development, as it does not require following task instructions. In infants, rs-EEG protocols usually consist of paying attention to an external source of stimulation (e.g., soap bubbles or stimuli presented on a screen), which helps them to stay as calm as possible (Anderson & Perone, 2018; Bell, 1998; Saby & Marshall, 2012).

Resting state EEG provides several measures, ranging from signal energy to connectivity measures. However, the gold-standard measurement in infant rs-EEG consists of decomposing the signal to extract the power in canonical frequency bands: theta (3–6 Hz), alpha (6–9 Hz), beta (9–20 Hz), and gamma (+20 Hz; Saby & Marshall, 2012). The power of each frequency band can be obtained in absolute terms (i.e., the actual value obtained for a particular frequency) or in relative terms, when the energy of a particular frequency is divided by the power of the rest of the signal or frequency bands (e.g., theta–beta ratio; Anderson & Perone, 2018; Saby & Marshall, 2012; Trujillo et al., 2019).

When the development of rs-EEG has been explored during the first years of life, relative power is more sensitive than absolute power because absolute power can be affected by skull changes over the lifespan (e.g., Marshall et al., 2002). Indeed, the transition from infancy to toddlerhood is a period of rapid reconfiguration of relative power in all the frequency bands. There is evidence that theta relative power is higher in younger infants. Also, a peak of activity in the infant alpha range emerges around the fourth month of life. Alpha peak appears as a sudden energy "bump" between 5 and 7 Hz, moves toward higher frequencies, and augments its relative power with age during the first years of life (Clarke et al., 2001; Gasser et al., 1988; MacNeill et al., 2018; Orekhova et al., 2006; Stroganova et al., 1999; Whedon et al., 2020). Furthermore, the alpha band relative power appears to show within-individual stability along infancy (Marshall et al., 2002). Finally, although research on higher frequency bands in infants is still scarce, a study by Tierney et al. (2012) suggests a reduction in frontal beta and gamma between the fifth month and the second year of life. Importantly, the relative power in different frequency bands appears to be related to individual differences in cognitive development (Anderson & Perone, 2018; Bell & Wolfe, 2007; Benasich et al., 2008; MacNeill et al., 2018; Perone et al., 2018; Whedon et al., 2020) as well as infants' risk of neurodevelopmental disorders (Arns et al., 2013; Begum-Ali et al., 2022; Gabard-Durnam et al., 2019; Tierney et al., 2012), which speaks for the relevance of understanding the early development of EEG activity at rest.

Although previous research suggests that relative power is sensitive to developmental changes, it only considers the energy of standard frequency bands that do not separate the background activity (aperiodic) from the periodic brain activity (Donoghue, Haller, et al., 2020; He, 2014; Ostlund et al., 2022; Voytek & Knight, 2015). In fact, the EEG power is a composite of a 1/f-like curve that accounts for most of the signal (aperiodic background) with some "bumps" or peaks that appear over it (periodic or oscillatory activity). More specifically, the aperiodic background curve has been defined with two parameters: offset (power at the lowest frequency of the aperiodic curve) and the slope or exponent of the curve. On the contrary, periodic brain activity refers to the frequency of the peaks and the energy above the aperiodic curve.

As a result of this conceptualization of EEG power, some authors argue that developmental variations of absolute and relative power can be due to changes in either aperiodic or periodic components of the EEG (Donoghue, Dominguez, et al., 2020; Ostlund et al., 2022; Samaha & Cohen, 2022). Consequently, different research groups have examined the maturation of aperiodic and periodic components (e.g., Cellier et al., 2021). In infancy, recent research has shown an aperiodic background curve in asleep newborns that flattens from birth to the seventh month of life (i.e., reduction in the exponent; Fransson et al., 2013; Schaworonkow & Voytek, 2021). This pattern is constant as the aperiodic power curve becomes flatter from age 3 years onward (Donoghue, Haller, et al., 2020; Hill et al., 2022; McSweeney et al., 2021; Voytek et al., 2015). Interestingly, the aperiodic parameters have been linked to cognitive processes and neurodevelopmental disorders, which accounts for their biological importance (Demuru & Fraschini, 2020; Immink et al., 2021; Karalunas et al., 2022; Shuffrey et al., 2022). Regarding the periodic components of EEG, studies have focused on

the alpha frequency band. Alpha peak frequency and the number of alpha bursts increase in the first year of life (Schaworonkow & Voytek, 2021) and during childhood, which suggest a rapid reconfiguration of periodic brain activity (e.g., Cellier et al., 2021).

Previous research points out that the development of relative power parallels changes in periodic and aperiodic components of the EEG. Consequently, both types of activity likely underlie age-related changes in relative power. Nevertheless, further research is needed to unveil the relationship between relative power and the aperiodic and periodic components, as well as the differential trajectories and stability of the signal in unexplored periods of the lifespan, such as the transition between infancy and toddlerhood. For this reason, we recorded rs-EEG in a longitudinal sample of infants who were evaluated in three different waves (at 6, 9, and 16 to 18 months of age) and computed the relative power of canonical frequency bands, periodic brain activity, as well as the offset and exponent (aperiodic background curve parameters). Our objective was to compare the trajectories of relative power and periodic brain activity and age-related changes in the aperiodic components. Also, we examined the within-subject stability of the signal and analyzed whether the relative power was related to the aperiodic components and periodic power. We expected to replicate changes in relative power previously found in studies with infants. That is, a reduction in the relative power of theta and beta, but an increase in alpha's relative power. In addition, we hypothesized similar trajectories of the periodic brain activity and a reduction in the exponent with age. Also, we predicted that the measurements across waves would be correlated, indicating that rs-EEG measurements are stable in the transition between infancy and toddlerhood. Finally, we expected that the relative power captures both background and periodic brain activity, which would be relevant in the interpretation of future rs-EEG studies.

2 | METHOD

2.1 | Participants

Infants were recruited at the maternity hospital in the city of Granada (Spain). Families were informed about the study when babies were born. Those caregivers who expressed a willingness to be further informed were contacted when the babies were 6 months old. The initial sample consisted of 143 infants born at term (more than 36 gestational weeks and weight over 2.7 kg) and did not have any family history of neurodevelopmental disorder (i.e., first and second-order relatives with a formal diagnostic). Participants were followed up in a second session at age 9 months ($n = 123$) and a third session at age 16 to 18 months ($n = 93$). Most of the third session of data collection took place at the time of the COVID-19 pandemic. As requested by the health authorities of the country, the activity of the laboratory ceased for a period of 4 months. As consequence, the age of the third session was extended from 16 to 18 months to facilitate the continuity of participants in the study. We will refer to it as the 16-mo. session hereon. The sample included in the analyses varied according to the method required for testing each hypothesis. For instance, the trajectory changes included the three waves in the model, whereas stability analyses were done in pairs (e.g., 6-month-old correlated to the 9-month-old session). Further details can be found in Supporting Information Tables S1–S3 (see Section 2.4. Data Analysis).

2.2 | Procedure

The rs-EEG protocol reported in this article is part of a larger longitudinal study, which included other age-adapted protocols (eye-tracking tasks in all the sessions and different behavioral protocols at the 9-month-old and 16-month-old sessions) conducted before the EEG recording. Data on other tasks and protocols will not be reported in this article. Including all protocols, the approximated duration of the session was 30 minutes (6 months old) or 1 hr (9 months old and 16 months old) including resting times between tasks, as well as setting up of the EEG acquisition net. The rs-EEG consisted of two 2-minute blocks. In the first block, the experimenter blew soap bubbles in front of the baby, whereas the second block consisted of a video displaying geometrical shapes and colors accompanied by soft music. During both periods of EEG acquisition, babies were seated on the parent's lap and the parents were instructed to hold the baby comfortably, remain silent, and not interact with the infant during the tasks.

2.3 | Electroencephalogram

2.3.1 | EEG recording

We recorded EEG brain activity using a high-density geodesic net (128 channels) and the software Net Station 4.3 (EGI Geodesic Sensor Net, Eugene, OR). The resting protocol was programmed and synchronized to Net Station with E-Prime 2.0. The signal was digitalized at 1000 Hz frequency, filtered using an elliptical lowpass (100 Hz) and high pass (0.1 Hz) hardware filters, and online reference to the vertex. The baby was also video recorded in synchrony with the EEG acquisition. This video was

used for posterior visual inspection to detect fragments in which the baby was fussy and/or there was a parental interruption (e.g., the parent talking to the baby and/or calling their attention). Those fragments were marked as invalid and were rejected from the analysis in the segmentation step (see Anderson et al., 2022).

2.3.2 | EEG processing

The pre-processing of the EEG signal was conducted with the EEGlab toolbox (Delorme & Makeig, 2004) with a combination of the Maryland Analysis of developmental EEG (MADE) pipeline (Debnath et al., 2020) and the Automated Pipeline for Infants Continuous EEG (APICE; Fló et al., 2022). The pre-processing steps are depicted in Supporting Information Figure S1.

First, we started with the MADE pipeline removing the boundary electrodes ($n = 20$; see Supporting Information Figure S2) as those were usually noisy. Then the continuous data set was filtered with a Hamming window (0.2–48 Hz) using a finite impulse response filter (FIR). The electrodes with constant noise along the EEG recording ("global bad channels") were identified and removed with the FASTER plug-in (Nolan et al., 2010) and excluded until the interpolation step. After removing those channels, a copy of the data set was performed and segmented into 1 s segments. The copied data set was high pass filtered (1 Hz) and cleaned from artifacts (threshold = ±1000 μV). Then, ICA was performed and independent components containing blinks or ocular movements were detected using infant adapted ADJUST plug-in (Leach et al., 2020). Those components were copied into the original data set and blink and eye-movement ICAs were removed from the signal.

Once the ICA components were removed, we employed the APICE pipeline over the continuum EEG signal to detect additional artifacts. This pipeline offers adaptive thresholds in several cycles based on the power spectrum, amplitude, variance, and amplitude transitivity of the signal, and marks a portion of the data as a "bad time" if more than 30% of the signal contain noise at that moment. Those "transient bad times" were then targeted with principal component analysis (see Yücel et al., 2014) and, in case there were shorter than 100 ms, the pipeline removed PCA components carrying up to 0.90 of the variances. After applying the PCA, we divided the signal into epochs of 2, 5, and 10 s and redefined the "transient bad times" with the previous parameters. That is to say, the pipeline evaluated the signal of each epoch to detect and mark the remaining "transient bad times." Epochs were considered noisy if they had more than 30% of bad channels or had more than the 30% of data interpolated within each segment. Then, the "global bad channels" were reintroduced and spherically interpolated, after which the signal was re-referenced to the average.

Over the remaining epochs, we applied a voltage threshold rejection of (±110 μV). If an electrode surpassed that value, it was marked as a bad electrode. In case that more than 20% of electrodes of an epoch crossed that threshold, the epoch was discarded. Finally, the signal was visually inspected and the segments with excessive noise were removed. Babies with less than 20 s of clean data or more than 10 "global bad electrodes" interpolated were discarded from further analysis ($n = 0$).

2.3.3 | Power computation: Frequency range, epoch length, and stimuli

We computed the absolute power employing the *spectopo* function in the toolbox EEGlab. The absolute power was computed with FFT in 0.1, 0.2, and 0.5 Hz steps for the 10, 5, and 2 s epochs, respectively. The power spectrum was extracted in incrementing ranges from 5 to 45 Hz in 5 Hz steps to determine the best fit of the aperiodic models (see below) and detect artifacts in high-frequency power. The aperiodic models fitted better when the gamma range was excluded (+21 Hz) due to a power bump in the gamma band range (i.e., motor artifacts; see Supplementary Material 1). Furthermore, employing a wide frequency range negatively affected the other frequency bands absolute error in the models. Therefore, we decided to focus on the 1–20 Hz frequency range (see Figure 1).

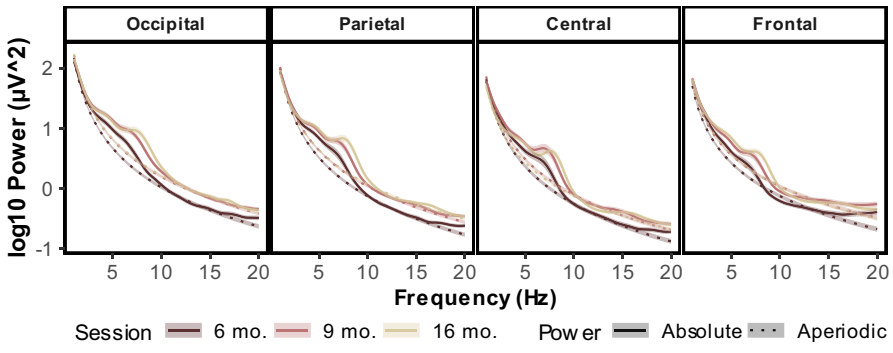

FIGURE 1 Mean and standard error (shaded area) of the absolute (solid) and aperiodic power (dotted) for each cluster of channels locations and age-session. The shaded area stands for twice the standard error.

Regarding the epoch length employed, we found that the 5 s division retained more infants in the analysis and had the same model fit in comparison with 2 s and 10s epochs. More importantly, the longitudinal results did not vary depending on the epochs and the within-participants stability improved probably due to the increase in the participant number (Supplementary Material 2). Therefore, for further analyses in the main text we used the data extracted with 5 s epochs. Also, the analysis in the main text included the data extracted from combining both resting blocks (bubbles and video) given the similarities of both conditions (both involved visual stimulation in the company of adults) and because it allowed the inclusion of more infants in the analyses than if we tested each block separately. Nevertheless, we also analyzed our hypotheses using data from bubbles and video separately and found similar results for the combined and separate blocks (see Section 2 of the Supplementary Material). However, some differences between blocks, mainly related to the theta band, were observed in some measurements within each age session. These differences are presented in Section 3 of the Supplementary Material.

2.3.4 | Aperiodic and periodic components of the EEG signal and relative power

The signal was decomposed into periodic and aperiodic components with the *specparam* toolbox (Donoghue, Haller, et al., 2020) called from EEGlab. The specparam toolbox models the absolute power of the signal in each frequency (P(f)) as a combination of aperiodic (L(f)) and periodic (G; Σn Gn (f)) components. The aperiodic component is defined as $L(f) = b - \log[fx]$ where b is a constant offset and χ is the aperiodic exponent. Notice that the exponent ($1/f^{x}$) is equivalent to the slope when transformed the power spectrum to log–log. However, for easiness, we will use the term "exponent" to refer to this parameter as we employ "slope" to describe the random effects in the longitudinal analysis (see Section 2.4. Data Analysis). The periodic contribution G is modeled as a Gaussian peak over the aperiodic curve. The parameters of the model were based on previous studies with infants (peak width limits: [2.5–12 Hz], the maximum number of peaks: 5, aperiodic mode: fixed, peak threshold: 2; see Schaworonkow & Voytek, 2021) and computed including the frequencies between 1 and 20 Hz. This range was larger than previous studies but necessary to compute the periodic brain activity including up to the beta frequency band. Only participants with $R^2 > .95$ were included in the model (Supporting Information Table S4). Once the aperiodic signal was obtained, it was subtracted from the absolute power to obtain the periodic power of the EEG activity. On the contrary, the relative power of each frequency band was computed by dividing the absolute power of each band by the power of all the frequency range employed (1–20 Hz).

2.3.5 | Frequency bands and clustering

As the frequency of each band changes along with development (Marshall et al., 2002), we decided to anchor the frequency bands initially to individual alpha frequency (IAF). However, after a visual inspection of individual power-spectrum plots, we found that infants had also a periodic peak in the theta range (around 4 Hz and increasing up to 4.5 Hz in the third session; see Supplementary Material 2). Therefore, we decided to anchor the periodic part of the signal based on both peaks, searching the theta peak between 3 and 5 Hz and the alpha peak between 6 and 9.5 Hz in the parieto-occipital clusters, a range usually employed in infants' studies (Marshall et al., 2002, Stroganova et al., 1999). The frequency bands were computed based on the full width at half maximum (FWHM) adjusting the frequency range to each infant. In all the cases, the beta band was constructed as 1.2*IAF-20 Hz as we did not find a clear beta peak (see Rayson et al., 2022, for comparable results with the periodic power). In case that a participant did not have a clear alpha or theta peak, we assumed the general range in infants: 3 to 5 Hz for theta and 6 to 9 Hz for alpha bands. The power was individually computed for each electrode and then average over the occipital, parietal, central, and frontal clusters (see Supporting Information Figure S2).

2.4 | Data analysis

2.4.1 | Longitudinal development of the EEG power and aperiodic parameters

As the attrition rate in developmental studies is high and missing data might bias the results, we employed maximum likelihood estimation in the analysis in children who came to at least two sessions (Enders, 2013; Graham, 2009; Matta et al., 2018). According to Littles' test, missing data were missing completely at random (MCAR; $\chi^2(7) = 4.80$, $p = .683$). Also, the infants who performed the second and third sessions did not differ in socioeconomic status (SES) from those who did not come to the laboratory either in the second ($t(101) = -0.60$, $p = .53$) or the third session ($t(101) = -0.37$, $p = .61$), which indicated that the estimation would not be affected by relevant environmental factors. As a result, we decided to analyze the data employing

linear mixed models estimating the missing data ($n = 101$; See Supporting Information Table S1).

The models included time and time squared (regressors) and cluster as fixed effects to predict relative/periodic power and the aperiodic components. We constructed the models following a bottom-up strategy, fitting first the random effects (random intercept, random slope of time, random slope of time by cluster) and then adding the fixed effects and their interaction (West et al., 2006). The models were compared with a chi-squared test for the goodness of fit with AIC. In case the residuals of the model were non-normally distributed, we employed the Tucker stair of ladders to transform the data and re-run the models from the first step. The degrees of freedom were computed using the Satterthwaite approximation. In the results, we report the effect size of both conditional and marginal with *r* squared (Nakagawa et al., 2017).

Contrary to other parameters in which we included all the channels in the analysis, in the alpha peak analysis we ran linear mixed models considering only the channels with a clear peak based on the *specparam* toolbox processing. Both variables, the percentage of electrodes with a clear alpha peak and the alpha frequency in the electrodes with the peak, were analyzed in the parieto-occipital cluster. The model included time and time squared to investigate linear and quadratic changes over time.

2.4.2 | Within-subjects stability of the parameters

To compute the stability between sessions, we ran two-tailed Spearman ranked correlations between each pair of sessions: 6–9, 6–9, and 9–16 without estimating the missing values ($n = 68$ in 6 to 9 months of age correlations; $n = 47$ in 6- to 16-month-old correlation; $n = 32$ in 9- to 16-month-old correlation).

2.4.3 | Contributions of aperiodic and periodic EEG components to relative power

To determine the contribution of periodic and periodic components of the EEG to the relative power, we ran and test three multilevel models from the simplest to more complex, introducing gradually the aperiodic and periodic components of the signal. The first model only included the intercept, the second one added the aperiodic parameters (offset and exponent), and the third introduced the periodic power. The goodness of the model was evaluated based on AIC and RMSE and the model with the lowest significant values in those parameters was selected. We decided to run a model for each session (6-, 9-, and 16 months old) and frequency band (theta, alpha, beta). We did not divide the regressions by cluster as we found that the correlation between the periodic and aperiodic parameters was constant independently of the electrode area (Supplementary Material 4).

3 | RESULTS

3.1 | Longitudinal development of the EEG power and aperiodic parameters

3.1.1 | Aperiodic components

The final model of the exponent included cluster, time, time squared, and the interaction time × cluster as fixed effects, as well as random slope overtime for each participant (marginal $r^2 = .38$, conditional $r^2 = .68$). The exponent diminished overtime (time: $\beta = -0.53$, $t(714.26) = -10.778$, $p < .001$, 95% CI = [−0.63, −0.43]), with a significant reduction in the change rate (time squared: $\beta = 0.38$, $t(579.03) = -7.030$, $p < .001$, 95% CI = [0.28, 0.49]). The exponent reduction was equal in the central and parietal clusters ($t < 1$). Nevertheless, the frontal ($\beta = 0.19$, $t(638.16) = 6.75$, $p < .001$, 95% CI = [0.13, 0.25]) and occipital ($\beta = 0.07$, $t(638.16) = 2.44$, $p = .015$, 95% CI = [0.01, 0.12]) clusters had a smaller reduction in comparison to the central and parietal clusters. Regarding the exponent value in the clusters, the frontal cluster had lower exponent values in comparison with all the clusters ($zs > 19.47$, all $ps < .001$), the occipital had higher exponent than the central and parietal clusters ($zs > 5.56$, all $ps < .001$), and the parietal had larger exponent than the central cluster ($z = 2.96$, $p = .019$).

The offset model included time, cluster, and the interaction time × cluster (marginal $r^2 = .54$, conditional $r^2 = .85$). The offset was not related to the session time ($t < 1$). However, the time factor interacted with the cluster, signaling different trajectories depending on the electrode area. The parietal and central clusters did not differ in the developmental trajectory ($\beta = 0.04$, $t(610.45) = 1.67$, $p = .09$, 95% CI = [−0.01, 0.09]) but the frontal ($\beta = 0.21$, $t(610.45) = 8.06$, $p < .001$, 95% CI = [0.16, 0.26]) and occipital ($\beta = 0.10$, $t(610.45) = 4.04$, $p < .001$, 95% CI = [0.05, 0.16]) clusters had larger change. Furthermore, the offset in the occipital cluster was more positive than the other clusters ($zs > 22.21$, all $ps < .001$), the parietal offset had higher values than the central and the frontal ($zs > 20.70$, $p < .001$), and the central area had larger offset than the frontal cluster ($z = 5.42$, $p < .001$). See Supporting Information Table S4 for the descriptive values of the offset and exponent measures and Figure 2 (average) and Supporting Information Figure S3 (individual clusters).

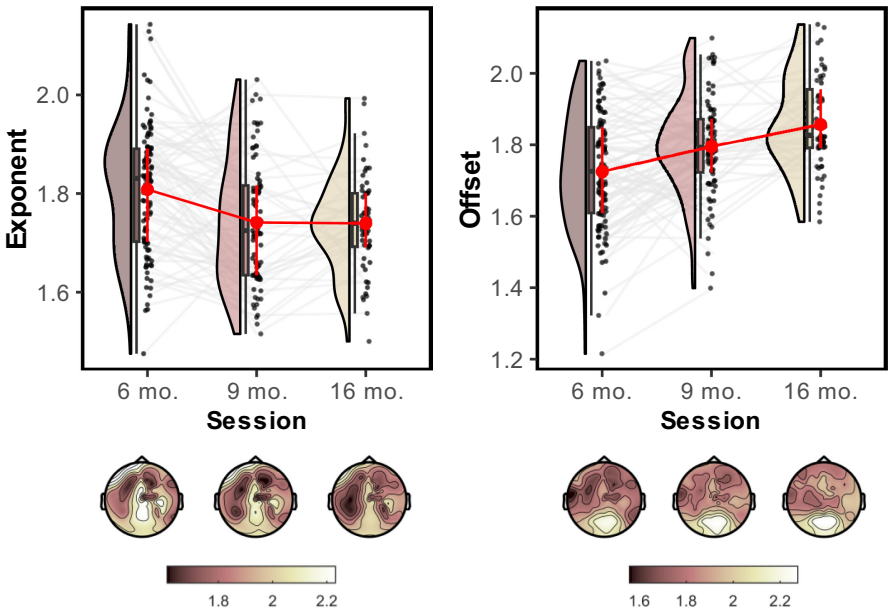

FIGURE 2 Development of the aperiodic components of the EEG signal for the average of all channels. The gray lines represent the trajectories of each individual, whereas the red line represents the group mean of the exponent (left) and offset (right). The bottom part of the figure shows the topographical distribution of these variables on the scalp.

TABLE 1 Descriptives of the alpha peak by cluster and session. It displays the proportion of channels with a peak (standard deviation) and the mean frequency of the peak (standard deviation) in those channels.

		Central		Frontal		Occipital		Parietal	
Session	**Sex**	**%**	**Freq.**	**%**	**Freq.**	**%**	**Freq.**	**%**	**Freq.**
6 months	F	0.91 (0.29)	7.01 (0.79)	0.68 (0.47)	6.81 (0.82)	0.91 (0.29)	6.96 (1.11)	0.87 (0.34)	7.00 (0.97)
	M	0.83 (0.37)	6.93 (0.92)	0.55 (0.5)	6.85 (0.91)	0.87 (0.33)	7.12 (1.2)	0.81 (0.39)	7.07 (1.03)
9 months	F	0.97 (0.18)	7.34 (0.6)	0.88 (0.32)	7.14 (0.71)	0.99 (0.09)	7.28 (0.78)	0.96 (0.2)	7.28 (0.7)
	M	0.88 (0.32)	7.27 (0.79)	0.68 (0.47)	7.07 (0.83)	0.95 (0.22)	7.31 (0.95)	0.92 (0.27)	7.31 (0.86)
16 months	F	1 (0.05)	7.96 (0.59)	0.97 (0.17)	7.83 (0.61)	1 (0)	7.8 (0.69)	0.99 (0.12)	7.90 (0.6)
	M	0.98 (0.14)	7.95 (0.73)	0.88 (0.33)	7.83 (0.88)	0.99 (0.08)	8 (0.64)	0.99 (0.09)	7.91 (0.69)

Note: The descriptives were extracted from the infants included in the linear mixed model analysis.

Abbreviations: F, female; M, male.

3.1.2 | Periodic brain activity

The descriptives for the periodic brain activity can be found in Table 1 (alpha peak), Supporting Information Table S5 (periodic power), and are displayed in Figure 3 and Figure 4 (top) for the average change across brain areas. The individual trajectories for each cluster can be seen in Supporting Information Figures S5 and S6.

Alpha peak

The percentage of electrodes with a clear peak in alpha increased from 85% to 99% across sessions (marginal $r^2 = .11$, conditional $r^2 = .27$). The change was quadratic, with faster increase in the first months in comparison with the following ones (time: $\beta = 0.46$, $t(142.57) = 3.75$, $p < .001$, 95% CI = [0.22, 0.71]; time squared: $\beta = -0.36$, $t(153.29) = -2.54$, $p = .012$, 95% CI = [−0.64, −0.08]). Regarding the individual alpha frequency, it varied significantly from 7.07 Hz in the first session to 7.89 Hz in the third session (marginal $r^2 = .26$, conditional $r^2 = .56$, $\beta = 1.03$, time: $t(150.35) = 11.26$, $p < .001$, 95% CI = [0.85, 1.21]).

Theta periodic power

The final model for theta periodic power included the time, time squared, cluster, and the interaction area × cluster as fixed effects (marginal $r^2 = .30$, conditional $r^2 = .77$). The periodic power augmented in this period (time: $\beta = 0.99$, $t(389.41) = 2.59$, $p = .012$, 95% CI = [0.21, 1.77]) with an inverted-u trajectory (time squared: $\beta = -1.40$, $t(623.01) = -3.16$, $p = .002$, 95% CI = [−2.26, −0.53]). The parietal ($\beta = -0.40$, $t(667.4) = -1.96$, $p = .04$, 95% CI = [−0.79, −0.01]) and occipital ($\beta = -1.02$, $t(667.4) = -5.05$, $p < .001$, 95% CI = [−1.41, −0.62]) clusters had lower linear increase than the central and frontal areas. The frontal and central, as well as the parietal and occipital, did not vary in theta periodic power ($zs < 1$). However, the occipital and parietal had larger power in

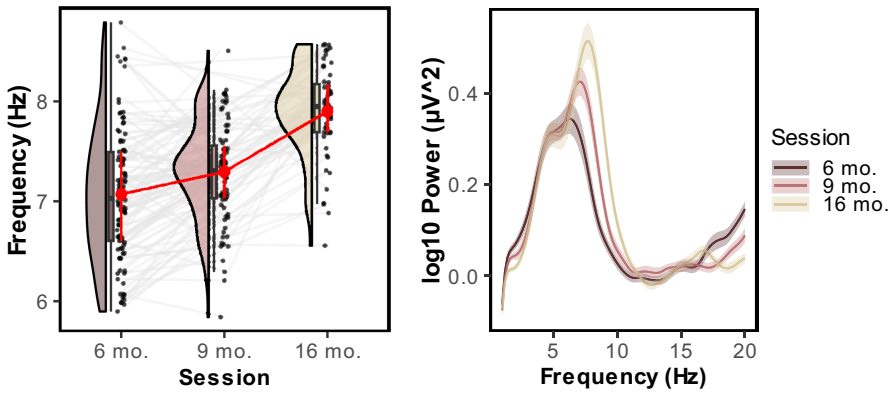

FIGURE 3 Mean peak frequency of the alpha peak (left) and periodic power (right) development in the parieto-occipital cluster. The figure displays the individual trajectory in gray as well as the average trajectory in red of alpha peak frequency. It also shows the periodic power (mean—solid line) and twice the standard error (shaded area) for each session.

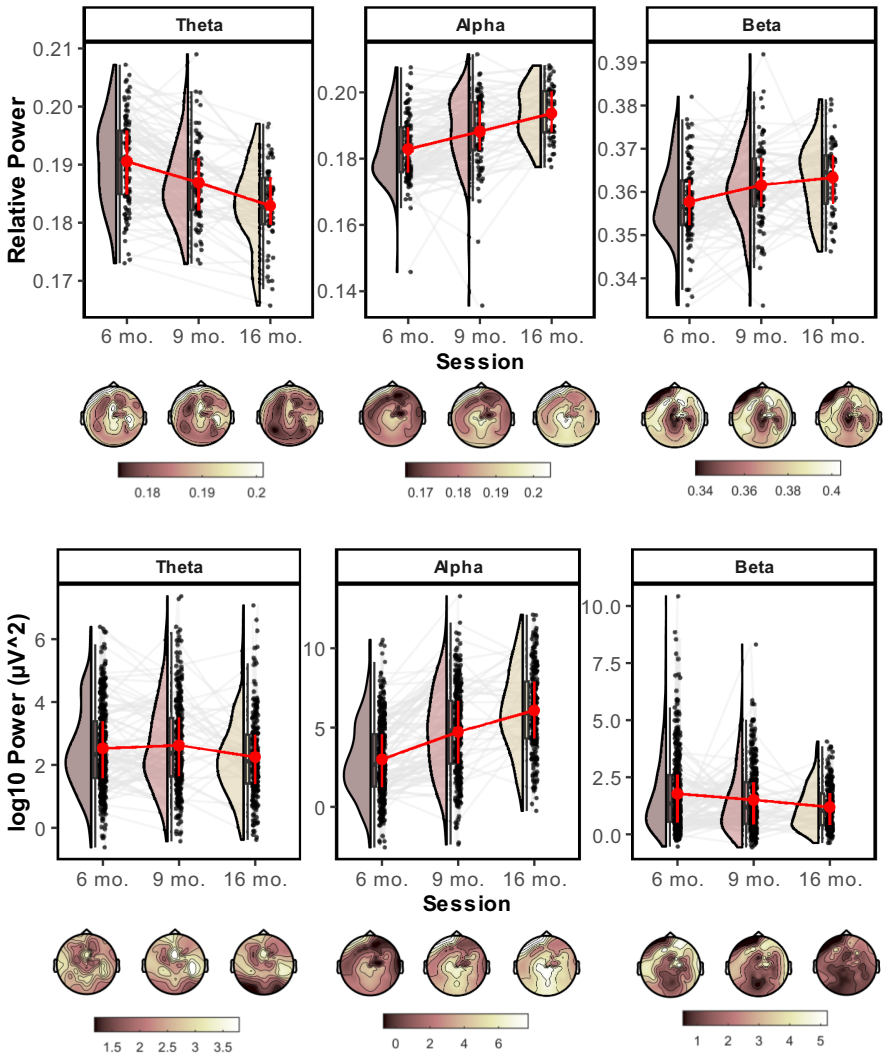

FIGURE 4 Relative (top) and periodic (bottom) power development on average and its topographical distribution. The gray bars of the raincloud plots display the individual trajectory, whereas the red line stands for the average trajectory.

comparison with the central ($zs > 3.85$, all $ps < .001$) and the frontal ($zs > 3.36$, all $ps < .001$) clusters.

Alpha periodic power

The model for alpha periodic power included time, time squared, and cluster as fixed effects (marginal $r^2 = .23$, conditional $r^2 = .86$). Alpha periodic power increased between sessions (time: $\beta = 9.35$, $t(266.39) = 13.796$, $p < .001$, 95% CI = [8.01, 10.68]) with slower change rate in the later months (time squared: $\beta = -7.38$, $t(744.8) = -9.74$, $p < .001$, 95% CI = [−8.87, −5,89]). The parietal, occipital, and central clusters did not differ in alpha periodic power ($zs < .2.157$, all $ps > .186$), but all the clusters had larger periodic power than the frontal area ($zs > 19.173$, all $ps < .001$).

Beta periodic power

The model for theta periodic power only included time and area as fixed effects (marginal $r^2 = .23$, conditional $r^2 = .86$). The frontal cluster had larger power compared with the other clusters ($zs > 14.54$, all $ps < .001$). Also, the central cluster exhibited more power than the occipital and parietal electrodes ($zs > 3.099$, all $ps < .012$), but the parietal had larger beta periodic power than the occipital cluster ($z = 2.84$, $p = .026$). The beta periodic power was reduced from the first session onward ($\beta = -0.69$, $t(27.74) = -3.43$, $p = .019$, 95% CI = [−1.11, −0.28]).

3.1.3 | Relative power

Relative power descriptives are displayed in Supporting Information Table S6 as well as Figure 4 (average) and Supporting Information Figure S7 (individual clusters).

Theta relative power

Theta relative power model fitted the best with linear and quadratic change plus area and area × time interaction (marginal $r^2 = .20$, conditional $r^2 = .77$). Theta relative power diminished over the sessions (time: $\beta = -0.02$, $t(457.13) = -8.74$, $p < .001$, 95% CI = [−0.03, 0.02]) and had a positive quadratic effect (time squared: $\beta = 0.01$, $t(532.14) = 4.75$, $p < .001$, 95% CI = [0.01, 0.02]), which signaled a rapid change followed by paced variation. The central cluster had reduced linear change in comparison with the frontal cluster ($\beta = -0.01$, $t(637.5) = -13.28$, $p < .001$, 95% CI = [−0.01, −0.01]) but no other trajectories differed ($ts < 2$). The central cluster had also larger relative power in theta than the rest of the clusters ($zs > 4.93$; all $ps < .001$), whereas the parietal had more power than the occipital and frontal clusters ($zs > 6.43$, $ps < .001$). The occipital and frontal cluster did not vary in theta relative power ($z = 2$, $p = .27$).

Alpha relative power

The alpha relative power model included time, time squared, and area as fixed effects as well as random slope for time in each participant (marginal $r^2 = .09$, conditional $r^2 = .88$). Relative power augmented along with the time (time: $\beta = 0.03$, $t(177.63) = 6.11$, $p < .001$, 95% CI = [0.02, 0.04]) with higher change rate in the first months (time squared: $\beta = -0.02$, $t(856.72) = -4.95$, $p < .001$, 95% CI = [−0.03, −0.01]). The parietal and occipital areas did not vary in alpha relative power ($z = 1.82$, $p = .412$) but both had larger power in comparison with the frontal cluster ($zs > 14.17$, all $ps < .001$). The central cluster had larger alpha relative power than the rest of the clusters ($zs > 4.585$, all $ps < .001$).

Beta relative power

The beta relative power model included time, time squared, and the interaction cluster × time as fixed effects (marginal $r^2 = .34$, conditional $r^2 = .59$). Relative power increased overtime (time: $\beta = 0.02$, $t(862.38) = 3.49$, $p < .001$, 95% CI = [0.01, 0.03]) with a negative quadratic effect (time squared: $\beta = -0.02$, $t(883.20) = -2.89$, $p = .004$, 95% CI = [−0.03, −0.01]). The frontal area had a paced change in comparison to the other clusters ($\beta = -0.01$, $t(838.49) = -3.65$, $p < .001$, 95% CI = [−0.02, −0.01]). The central cluster had lower power than the other clusters ($zs > 3.91$, all $ps < .001$). Furthermore, the relative power of the beta band was smaller in the parietal cluster than the frontal and occipital ones ($zs > 4.9$, all $ps < .001$). Also, the frontal area had larger power than the occipital cluster ($z = .14.48$, $p < .001$).

3.2 | Within-subjects stability of the parameters

3.2.1 | Aperiodic components

The exponent was correlated between the first and the rest of the sessions independently of the cluster employed ($r_s = [.41, .55]$, $ps < .01$). However, the correlations between 9- and 16-month-old sessions only were significant in the central cluster ($r_s = .56$, $p < .001$). The offset had the same pattern, with high stability between the first, and the second, as well as the first and third sessions in all the electrode areas ($r_s = [.36, .60]$, $ps < .001$) but with no significant correlation between the 9-month-old and 16-month-old sessions (see Table 2).

3.2.2 | Periodic brain activity

Alpha periodic power was stable independently of the cluster and session compared ($r_s = [.42, .64]$, $ps < .01$). Theta periodic power was also constant between the first and the second, as well as the first and third session ($r_s = [.12, .56]$, $ps < .05$), but with no relationship between the second and the third session. The beta band was not constantly related between sessions but in the frontal area (6- to 9 months old) ($r_s = [.29, .49]$, $ps < .05$). See Table 2.

3.2.3 | Relative power

Relative power in the three frequency bands was related between the first and the second and the first and the third sessions independently of the cluster ($r_s = [.36, .68]$, $ps < .05$). However, only alpha in general and theta in the

TABLE 2 Stability correlations between the three waves of the study for the aperiodic components and the relative and periodic power.

			Aperiodic components		Periodic power			Relative power		
Waves	**Cluster**	***n***	**Exponent**	**Offset**	**Theta**	**Alpha**	**Beta**	**Theta**	**Alpha**	**Beta**
6- to 9 months	Occipital	68	0.51***	0.45***	0.36***	0.54***	0.11	.32**	.55***	.36**
			[0.45–0.57]	[0.38–0.51]	[0.54–0.65]	[0.48–0.6]	[0.03–0.19]	[.24–.40]	[.49–.60]	[.29–.43]
	Parietal	68	0.48***	0.46***	0.43***	0.62***	0.09	.49***	.64***	.40***
			[0.41–0.54]	[0.39–0.53]	[0.52–0.63]	[0.56–0.67]	[0.01–0.18]	[.43–.56]	[.59–.69]	[.32–.46]
	Central	68	0.54***	0.53***	0.19***	0.64***	0.29*	.46***	.67***	.39**
			[0.48–0.6]	[0.47–0.59]	[0.39–0.52]	[0.59–0.69]	[0.21–0.36]	[.39–.52]	[.61–.71]	[.31–.46]
	Frontal	68	0.49***	0.42***	0.18***	0.48***	0.36**	.57 ***	.50 ***	.36 **
			[0.42–0.55]	[0.35–0.49]	[0.57–0.68]	[0.42–0.55]	[0.28–0.43]	[.52–.63]	[.44–.56]	[.39–.43]
6- to 16 months	Occipital	47	0.43**	0.36*	0.12*	0.51***	0.02	0.4**	.45**	0.37*
			[0.34–0.51]	[0.27–0.45]	[0.2–0.39]	[0.43–0.58]	[−0.09–0.12]	[0.31–0.48]	[.36–.52]	[0.28–0.45]
	Parietal	47	0.41**	0.5***	0.27**	0.47***	0.17	0.5***	.45***	0.41**
			[0.33–0.49]	[0.42–0.57]	[0.36–0.53]	[0.39–0.55]	[0.07–0.27]	[0.42–0.57]	[.37–.53]	[0.32–0.49]
	Central	47	0.55***	0.56***	0.51***	0.42**	0.43**	0.68***	.42**	0.57***
			[0.47–0.61]	[0.48–0.62]	[0.53–0.66]	[0.33–0.5]	[0.35–0.51]	[0.62–0.73]	[.33–.50]	[0.50–.63]
	Frontal	47	0.41**	0.6***	0.56***	0.45**	0.49***	0.63***	.43 **	0.45**
			[0.32–0.49]	[0.54–0.67]	[0.59–0.71]	[0.36–0.52]	[0.4–0.56]	[0.56–0.69]	[.34–.51]	[0.37–.53]
9- to 16 months	Occipital	32	0.15	0.31#	0.17	0.56***	0.02	0.16	.42*	0.11
			[0.03–0.27]	[0.19–0.42]	[0.15–0.38]	[0.47–0.64]	[−0.1–0.15]	[0.03–0.28]	[.31–.51]	[−0.01–0.23]
	Parietal	32	0.3#	0.14	0.53	0.45**	0.05	0.45**	.38*	0.19
			[0.18–0.41]	[0.01–0.26]	[0.18–0.4]	[0.35–0.55]	[−0.08–0.17]	[0.35–0.55]	[.26–.49]	[0.07–0.31]
	Central	32	0.56***	0.34#	0.15	0.48**	0.04	0.4*	.47**	0.09
			[0.46–0.64]	[0.23–0.45]	[−0.11–0.14]	[0.37–0.57]	[−0.08–0.17]	[0.29–0.5]	[.37–.56]	[−0.03–0.21]
	Frontal	32	0.34#	0.32#	0.17	0.55**	0.43*	0.42*	.53 **	0.07
			[0.22–0.45]	[0.2–0.42]	[0.05–0.29]	[0.46–0.63]	[0.33–0.53]	[0.31–0.52]	[.44–.62]	[−0.06–0.19]

Note: The table displays Spearman's rho value as well as 95% CI for the correlations.

*$p < .05$; **$p < .01$; ***$p < .001$;

#$p > .05$ & $p < .1$.

frontal and parietal clusters were related between the 9 and the 16 months ($r_s = [.38, .53]$, $ps < .05$; see Table 2).

3.3 | Relationship between relative and aperiodic and periodic activity

We conducted regression models to understand the contribution of periodic power and aperiodic components of the EEG signal to the relative power in all frequency bands. Information about these regression models is presented in Table 3.

3.3.1 | Theta

The models predicting theta relative power were significant in all the waves: 6 months old (adj. $R^2 = .76$, $F(3, 107) = 119.5$, $p < .001$), 9 months old (adj. $R^2 = .71$, $F(3, 71) = 62.14$, $p < .001$), 16 months old (adj. $R^2 = .68$, $F(3, 50) = 38.47$, $p < .001$). The predictors did not vary between sessions, being related positively to periodic power in the theta band ($\beta = [0.73, 0.75]$, $ps < .001$) and to the exponent of the aperiodic component ($\beta = [0.36, 0.39]$, $ps < .001$).

3.3.2 | Alpha

Regression models were significant in all the sessions (adj. $r^2 = [.59, .94]$, $ps < .001$). Independently of the session, the alpha models included the periodic power and the intercept as the only predictors (6 months old: $\beta = .81$, $t(107) = 12.87$, $p < .001$; 9 months old: $\beta = .81$, $t(71) = 10.28$, $p < .001$; 16 months old: $\beta = .98$, $t(50) = 29.1$, $p < .001$).

3.3.3 | Beta

Beta relative power was significantly predicted in the three waves (6 months old: adj. $r^2 = .62$, $F(3, 107) = 62.5$, $p < .001$; 9 months old: adj. $r^2 = .34$, $F(3, 71) = 13.93$, $p < .001$; 16 months old: adj. $r^2 = .62$, $F(3, 50) = 9.21$, $p < .001$). In all the sessions, the exponent negatively predicted the relative power ($\beta = [-0.39, -0.23]$, $ps < .05$), and the periodic power was positively related to the relative power ($\beta = [0.37, 0.60]$, $ps < .001$). The offset only significantly predicted the relative power in the first session ($\beta = -0.27$, $p < .001$).

4 | DISCUSSION

The goal of the present study was to understand the developmental trajectory of relative power, periodic power, and aperiodic components and test its stability in a baseline rs-EEG in infants. Also, we evaluated the contributions of periodic power and aperiodic background parameters to relative power. Our results replicated previous results (e.g., reduction in theta relative power) and expanded previous findings in relative suggesting differential developmental curves when the power is isolated from the aperiodic background. Additionally, the measures were stable across sessions, signaling a large stability of the energy in the first months of life. This result shed further light on the development of rs-EEG power in infancy extending previous knowledge on the early development of EEG activity. Furthermore, the relative power was related to the aperiodic components in theta and beta frequency bands, but not in the alpha frequency band, which indicates that EEG relative power in the theta and beta bands captures a combination of both periodic and aperiodic brain activity.

4.1 | EEG power: Development, stability, and relationship

4.1.1 | Aperiodic components

The offset did not change with age in our study in the 1 to 20 Hz range and linear trajectories were highly dependent on the epoch and maximum frequency range. On the contrary, the exponent decreased with age in the three waves, slowing down the reduction change over time independently of the frequency range, condition, and epoch (see Supplementary Material 2). This supports previous results in infants and children, as well as the initial hypothesis, and signals a marked trajectory in the first years of life (e.g., Cellier et al., 2021; Donoghue, Dominguez, et al., 2020; Hill et al., 2022; McSweeney et al., 2021; Schaworonkow & Voytek, 2021; Voytek et al., 2015). Thus, our results indicate that the aperiodic background curve flattens between 6 months and 18 months of age (i.e., the aperiodic curve power decays slower in older children). This suggests a change toward more excitatory activity in the excitatory/inhibitory balance (Gao et al., 2017; Voytek & Knight, 2015). Interestingly, the exponent and the offset displayed an anterior–posterior pattern, with larger intercepts in the posterior areas and a steeper aperiodic power curve. Moreover, the measures were stable, and the exponent and the offset were good predictors of infant values in later sessions.

In this interpretation, is worth mentioning the preprocessing steps and the stimuli employed in the study. In relation to the protocol variances between investigations, rs-EEG studies in infants vary in the images that are presented and the general protocol. This is a well-known factor that impacts on electrophysiological

TABLE 3 Regression analysis assessing the contribution of the aperiodic components and periodic activity to relative power of each frequency band.

Band	Session	Variable	*df*	R^2	Adj. R^2	RMSE	*F*	95% CI	*β*	*t*
Theta	6 months	Model	3, 107	.77	.76	0.004	119.5***			
		Offset						[−0.20, 0.03]	−0.08	−1.46
		Exponent						[0.27, 0.50]	0.39	6.70***
		Periodic						[0.66, 0.85]	0.75	15.90***
	9 months	Model	3, 71	.72	.71	0.004	62.14***			
		Offset						[−0.26, 0.05]	−0.10	−1.32
		Exponent						[0.22, 0.51]	0.36	4.89***
		Periodic						[0.64, 0.91]	0.78	11.55***
	16 months	Model	3, 50	.70	.68	0.004	38.47***			
		Offset						[−0.21, 0.18]	−0.02	−0.19
		Exponent						[0.19, 0.58]	0.38	3.95***
		Periodic						[0.57, 0.89]	0.73	9.33***
Alpha	6 months	Model	3, 107	.62	.61	0.008	58.74***			
		Offset						[−0.24, 0.07]	−0.01	−1.08
		Exponent						[−0.05, 0.25]	0.10	1.29
		Periodic						[0.69, 0.94]	0.81	12.87***
	9 months	Model	3, 71	.61	.59	0.009	36.99***			
		Offset						[−0.27, 0.10]	−0.09	−0.94
		Exponent						[−0.13, 0.24]	0.05	0.60
		Periodic						[0.64, 0.95]	0.80	10.28***
	16 months	Model	3, 50	.95	.94	0.002	307.5***			
		Offset						[−0.07, 0.10]	0.01	0.34
		Exponent						[−0.06, 0.10]	0.02	0.58
		Periodic						[0.91, 1.05]	0.98	29.10***
Beta	6 months	Model	3, 107	.63	.62	0.007	62.5***			
		Offset						[−0.41, −0.12]	−0.27	−3.69***
		Exponent						[−0.37, −0.09]	−0.23	−3.16***
		Periodic						[0.48, 0.72]	0.60	10.18***
	9 months	Model	3, 71	.37	.34	0.009	13.93 ***			
		Offset						[−0.38, 0.09]	−0.15	−1.26
		Exponent						[−0.49, −0.05]	−0.27	−2.40*
		Periodic						[0.23, 0.62]	0.43	4.30***
	16 months	Model	3, 50	.36	.32	0.007	9.21***			
		Offset						[−0.43, 0.16]	−0.13	−0.93
		Exponent						[−0.68, −0.10]	−0.39	−2.71**
		Periodic						[0.13, 0.60]	0.37	3.13**

*$p < .05$; **$p < .01$; ***$p < .001$.

brain activity (e.g., John et al., 2016). Indeed, in comparison with adults and children (usually eyes open vs. eyes closed) our study and other studies with infants usually present visual and/or auditive stimulation to calm the infants and reduce their movements (Saby & Marshall, 2012; see also Anderson et al., 2022). This might affect the developmental change, as it has been found in other studies (Hill et al., 2022). Indeed, the offset did change concurrently between our two block conditions (see Supplementary Material 3), suggesting an impact of the stimuli presented and/or the EEG variation along the session. However, the results in the developmental changes in our study were similar between conditions and when the different stimuli (video vs. bubbles) were

introduced altogether (see Supplementary Material 2). It is possible that the resemblance between blocks (i.e., visual and auditory stimuli) resulted in similar trajectories, whereas eyes open versus eyes close paradigms remove the visual information in the later condition. This is in line with the findings of Jacob et al. (2021) in adults, which unveiled that the aperiodic parameters were related to the hemodynamic changes in the auditory salience network in a simultaneous fMRI-EEG recording, and suggest the sensibility of aperiodic EEG signal to contextual change.

4.1.2 | Periodic and relative power

Contrary to our general prediction of similar development of relative power and periodic power, the development of relative compared with periodic power displayed variations in theta and beta and only was similar in the alpha band. First, the relative power in theta diminished between 6- and 18 months old, whereas the periodic power augmented in general in this period to rapidly decay. Similarly, beta relative power increased with age, while the periodic power diminished in the same period. Conversely, alpha frequency bands showed the same pattern of age-related change for both relative and periodic power. Additionally, the channels with a clear alpha peak augmented, which came with an increment in the frequency of the alpha peak of nearly 1 Hz.

The developmental trajectories in relative power were like previous experiments with infants: reduction in theta relative power and increment of alpha relative power (e.g., Marshall et al., 2002; Orekhova et al., 2006; Stroganova et al., 1999). However, beta results differed from other studies that have found an augment of absolute power (Wilkinson et al., 2023) but are similar to Tierney et al. (2012). One difference is the nature of the power (absolute vs. relative) as well as the range employed (we removed from 21 Hz onwards), which signals the necessity of more fine-grained measurements to capture infant electrophysiological development (see Section 4.3. Limitations and Future Directions). Indeed, when we isolated the periodic brain activity by removing the aperiodic background, only alpha had the same results than previous experiments (e.g., Marshall et al., 2002). Furthermore, the observed increment of periodic power in alpha is consonant with previous studies with periodic power in younger infants, as Schaworonkow and Voytek's (2021) found an increment of alpha burst presence over the first 7 months of life. Also, the alpha peak found after removing the background activity remains in the range called "infant alpha" (6–9 Hz; Orekhova et al., 1999, 2001, 2006; Stroganova et al., 1999), and it will probably transit to adult frequencies around the seventh year of life (Cellier et al., 2021). Finally, one similarity that our results had between relative power and periodic power was the quadratic component of the developmental changes. In general, the power changed faster in the first months to slow down the change rate in the following ones. This supports the notion of two developmental periods with different developmental slopes in each one as a recent study has shown with the absolute power (Wilkinson et al., 2023).

Electroencephalography power measures were stable in the transition between infancy and toddlerhood. That is to say, the relative power in previous sessions was a predictor of the following ones, especially in theta and alpha bands. On the contrary, periodic power in earlier sessions predicted the follow-up ones to a lesser extent than the relative power except for the alpha band. For instance, beta periodic had no consistent relationship over the sessions, whereas the relative power had at least good predictability between 6- and 9-month-old sessions (see Supporting Information Figures S13 and S14). Considering this, rs-EEG measures might be considered a fingerprint of the individual brain activity, combining both change and stability across the development regarding aperiodic parameters and power in theta and alpha bands. These results are consistent with previous research showing the stability of alpha relative power between 10 months old and 14 months old, and between 14 months old and 24 months old, but not between 5 and 10 months of age (Marshall et al., 2002). These differences might be due to the increase in the first session age (from 5- to 6 months old), which suggests that the EEG becomes more stable in this period. However, another plausible explanation is how we computed the frequency ranges of each band. We focused on the alpha and theta peaks trying to capture the interindividual variability present in our sample. For this reason, we computed an area around the peak based on the FWHM of each peak and infant with a resolution of 0.2 Hz (main text). This might have contributed to find the stability between sessions as the frequency range is not a fixed interval around the peak but rather focuses on the Gaussian shape above the aperiodic components individually. Indeed, the Gaussian width changes depending on the burst and rhythmic properties of a frequency (van Ede et al., 2018). Thus, adapting the peak range for each participant also considers the type of oscillation underlying the power spectrum to some extent.

The fact that the relative power was more stable than the periodic power might be due to two distinct factors. First, it is possible that the ratio between the bands remains constant along with the development, apart from maturational aspects. Second, it is also plausible that the

relative power is stable because it involves both periodic and aperiodic components of the EEG. In our study, the aperiodic components in the first sessions were good predictors of the following ones. Supporting the last idea, a recent study by Demuru and Fraschini (2020) showed that the aperiodic parameters of the signal are sensitive to individual variations in adults, which points out the distinctiveness of EEG aperiodic components. Thus, our data suggest that both exponent and offset might have contributed to the stability and therefore can be considered a relevant interindividual factor.

Last, the lack of correlations between the 9-month-old and 16-month-old sessions might be due to the sample size of those analyses. There were more significant correlations between the 6- and the 16-month-old infants than between the 9- and 16-month-old. As it is unlikely that the stability appears and reappears, the reduction in the sample size (i.e., $n = 32$) might have impacted the correlations.

Finally, and more importantly, we have shown that the relative power is a mixture of both aperiodic and periodic components in most of the frequency bands. For instance, theta and beta relative power was predicted by the exponent parameter. Only alpha was explained by periodic power without the contribution of other aperiodic components of the signal. What is more, alpha relative power was not directly correlated to the exponent and offset in any cluster and age but in the frontal cluster at the 6-month-old session with the offset (see Supplementary Material 4). Therefore, relative power captures to some extent the oscillations above the aperiodic background activity, but it is usually a mixture of the aperiodic and periodic power. Indeed, the contribution of periodic power and aperiodic parameters was usually equal in the theta and beta bands (Supporting Information Figures S17 and S18), supporting the relevance of both exponent and offset in the EEG signal. These results are consonant with previous research conducted by Donoghue, Dominguez, et al. (2020). They compared the correlation between aperiodic parameters and the periodic power to several power ratios (e.g., theta/beta) with data from the Multimodal Resource for Studying Information Processing in the Developing Brain (MIPDB). They found that alpha ratios were more correlated to the direct power of alpha than the aperiodic parameters, but the opposite pattern emerged when the ratios did not include the alpha frequency band (e.g., theta/beta). Altogether, this shows the relevance of considering the aperiodic components when working with EEG power. Furthermore, it indicates that alpha power might be biasing the results of the rest of frequency bands when computing relative power. That is to say, the large increment in alpha energy observed in early development probably overshadows age-related changes in the periodic power of other frequency bands when using the relative power.

4.2 | EEG power development and neurodevelopmental disorders

As the relative power contains combines aperiodic and periodic brain activity, previous brain–behavior relationships can be driven by any of them, which could have impacted the replicability between studies (Donoghue, Haller, et al., 2020; Voytek & Knight, 2015). Thus, separating the EEG signal into aperiodic and periodic components provides a way to explore their possible separate impact.

One example is the theta/beta ratio concerning ADHD (Liechti et al., 2013; Ogrim et al., 2012). For instance, recent studies showed that a higher theta/beta ratio was related to a higher risk of ADHD in 10-month-old infants (Begum-Ali et al., 2022). However, Karalunas et al. (2022) found that 1-month-old infants with ADHD risk had a steeper aperiodic background (i.e., larger exponent). Also, the relationship between aperiodic components and ADHD in adolescents was sensitive to whether the participant had taken medication and the exponent varied in comparison with their peers (Ostlund et al., 2021; Robertson et al., 2019). Therefore, aperiodic parameters are also affected in ADHD and are sensitive even to intervention.

Another of the most studied relationships between EEG and neurodevelopmental disorders is between ASD and relative or absolute power. However, to date, the findings are contradictory sometimes and malleable with development. For instance, a review published in 2013 points out an augment of low frequencies power, beta, and gamma, but a reduction in alpha power in the population diagnosed or with risk of ASD (Wang et al., 2013). However, other studies in younger participants signals a reduction in gamma in infants at risk of ASD, probably due to different maturational trajectories (Gabard-Durnam et al., 2019; Tierney et al., 2012). Thus, as the effects are related to gamma and beta, it is possible that the aperiodic components would be related to ASD. Indeed, a recent study by Shuffrey et al. (2022) supports this idea. In their study, they found that infants' EEG aperiodic exponent at birth was related to later ASD symptoms, whereas absolute power was not associated with ASD symptomatology. Therefore, aperiodic parameters seem to be related to developmental disorders, and in combination with the results of the current study, signal the importance of considering aperiodic components of the EEG signal when it comes to understanding the electrophysiological bases of neurodevelopmental disorders.

4.3 | Limitations and future directions

The current study focused on the early development of relative power in different frequency bands and the possible contribution of aperiodic and periodic in the standard frequency bands up to beta (1–20 Hz). Thus, our range is narrower than the ones employed in adult and children's studies. The decision of excluding gamma was related to the presence of artifacts in its frequency range found in the absolute power measurement (see Supplementary Material 1). Indeed, the parametrization of the aperiodic curve was affected by the presence of gamma, which (1) resulted in a reduction in the fit, especially in the frontal electrodes, (2) changed the values of the exponent and offset, and (3) increased the error of the model in the other frequency bands. This is a constant problem in studies with awake infants. For instance, Schaworonkow and Voytek (2021) found the best results in the range from 1 to 10 Hz. In contrast, studies with asleep infants (Fransson et al., 2013) were not as affected by the movements, which reveals the difficulty of the study. Thus, further experiments should seek conditions that reduce to a greater extent the motion and explore the gamma band in awake infants.

Concerning the pre-processing, we wanted to compare the periodic oscillations and relative power in an equivalent way to traditional approaches. Therefore, we decided to compute periodic power as we did in the relative power: anchoring the frequency bands to theta and alpha peak frequencies. However, future studies would benefit from finding each frequency peak with even more advanced techniques (Cohen, 2021; Ostlund et al., 2022). Also, especially in infancy, oscillatory brain activity seems to appear in bursts and is not sustained over time in some frequencies (e.g., beta band—Rayson et al., 2022). Therefore, assessing the presence of those bursts and computing the power with them would increase the reliability of results and give other parameters of interest, especially in frequency bands that usually lack a clear peak (Cole & Voytek, 2019; Ostlund et al., 2022). Finally, as infants' protocols incorporate an active baseline, recording peripheral and behavioral measures related to infants' cognitive state could give us information and increase the comparability between infant's and other developmental studies (e.g., Xie et al., 2018).

5 | CONCLUSION

Computing relative power is one of the most common analysis approaches to studying rs-EEG signals in infants. Patterns of the relative power of different frequency bands show fast changes in the early years of life and are associated with cognitive development and neurodevelopmental disorders risk. Although it is usually assumed that relative power represents neural oscillations, the EEG signal combines both aperiodic and periodic components. Our results indicate that, at least in the transition from infancy to toddlerhood, relative power is partially driven by changes in aperiodic activity. Therefore, relative power seems to capture both aperiodic and periodic components of the EEG power instead of the putative oscillations of EEG. This signals the necessity to incorporate more fine-grained measurements of EEG power to unveil the mechanism underlying brain maturation and its relation to cognitive processes.

AUTHOR CONTRIBUTIONS

Josué Rico-Picó: Conceptualization; data curation; formal analysis; investigation; methodology; visualization; writing – original draft; writing – review and editing. **Sebastián Moyano:** Investigation; writing – review and editing. **Ángela Conejero:** Investigation; methodology; supervision; writing – review and editing. **Ángela Hoyo:** Investigation; writing – review and editing. **M. Ángeles Ballesteros:** Investigation. **M. Rosario Rueda:** Conceptualization; funding acquisition; project administration; supervision; writing – review and editing.

ACKNOWLEDGMENTS

This study was funded by two grants from the MCIN/AEI/10.13039/501100011033 (ref. PID2020-113996GB-I00 and PSI2017-82670-P) awarded to MMR. The work of the first author was supported by a fellowship from the Fundación Tatiana in Neuroscience. We would also like to thank all the families that participated in the study over these years.

DATA AVAILABILITY STATEMENT

Due to the sensitivity of the data of the study, data are available on request to MR (rorueda@ugr.es). All the code is available on request to JR (rpicoj@ugr.es).

ORCID

Josué Rico-Picó https://orcid.org/0000-0001-6826-3569
Sebastián Moyano https://orcid.org/0000-0002-4612-2770
Ángela Conejero https://orcid.org/0000-0001-7323-6805
Ángela Hoyo https://orcid.org/0000-0003-4868-888X
M. Rosario Rueda https://orcid.org/0000-0002-3941-9031

REFERENCES

Anderson, A. J., & Perone, S. (2018). Developmental change in the resting state electroencephalogram: Insights into cognition

and the brain. *Brain and Cognition*, *126*, 40–52. https://doi.org/10.1016/j.bandc.2018.08.001

Anderson, A. J., Perone, S., & Gartstein, M. A. (2022). Context matters: Cortical rhythms in infants across baseline and play. *Infant Behavior and Development*, *66*, 101665. https://doi.org/10.1016/j.infbeh.2021.101665

Arns, M., Conners, C. K., & Kraemer, H. C. (2013). A decade of EEG theta/Beta ratio research in ADHD: A meta-analysis. *Journal of Attention Disorders*, *17*(5), 374–383. https://doi.org/10.1177/1087054712460087

Begum-Ali, J., Goodwin, A., Mason, L., Pasco, G., Charman, T., Johnson, M. H., & Jones, E. J. H. (2022). Altered theta–beta ratio in infancy associates with family history of ADHD and later ADHD-relevant temperamental traits. *Journal of Child Psychology and Psychiatry*, *63*, 1057–1067. https://doi.org/10.1111/jcpp.13563

Bell, M. A. (1998). The ontogeny of the EEG during infancy and childhood: Implications for cognitive development. In B. Garreau (Ed.), *Neuroimaging in child neuropsychiatric disorders* (pp. 97–111). Springer.

Bell, M. A., & Wolfe, C. D. (2007). The use of the electroencephalogram research on cognitive development. In L. A. Schmidt, & S. J. Segalowitz (Eds.), *Developmental psychophysiology: Theory, systems, and methods* (pp. 150–170). Cambridge University Press. https://doi.org/10.1017/CBO9780511499791.008

Benasich, A. A., Gou, Z., Choudhury, N., & Harris, K. D. (2008). Early cognitive and language skills are linked to resting frontal gamma power across the first 3 years. *Behavioural Brain Research*, *195*(2), 215–222. https://doi.org/10.1016/j.bbr.2008.08.049

Buzsáki, G. (2006). *Rhythms of the brain*. Oxford university press.

Buzsáki, G., Anastassiou, C. A., & Koch, C. (2012). The origin of extracellular fields and currents—EEG, ECoG, LFP and Spikes. *Nature Reviews Neuroscience*, *13*(6), 407–420. https://doi.org/10.1038/nrn324

Buzsáki, G., & Draguhn, A. (2004). Neuronal oscillations in cortical networks. *Science*, *304*(5679), 1926–1929. https://doi.org/10.1126/science.1099745

Cellier, D., Riddle, J., Petersen, I., & Hwang, K. (2021). The development of theta and alpha neural oscillations from ages 3 to 24 years. *Developmental Cognitive Neuroscience*, *50*, 100969. https://doi.org/10.1016/j.dcn.2021.100969

Clarke, A. R., Barry, R. J., Mccarthy, R., & Selikowitz, M. (2001). Age and sex effects in the EEG: Development of the normal child. *Clinical Neurophysiology*, *112*(5), 806–814. https://doi.org/10.1016/S1388-2457(01)00488-6

Cohen, M. X. (2017). Where does EEG come from and what does it mean? *Trends in Neurosciences*, *40*(4), 208–218. https://doi.org/10.1016/j.tins.2017.02.004

Cohen, M. X. (2021). A data-driven method to identify frequency boundaries in multichannel electrophysiology data. *Journal of Neuroscience Methods*, *347*, 108949. https://doi.org/10.1016/j.jneumeth.2020.108949

Cole, S., & Voytek, B. (2019). Cycle-by-cycle analysis of neural oscillations. *Journal of Neurophysiology*, *122*(2), 849–861. https://doi.org/10.1016/j.jneumeth.2020.108949

Debnath, R., Buzzell, G. A., Morales, S., Bowers, M. E., Leach, S. C., & Fox, N. A. (2020). The Maryland analysis of developmental EEG (MADE) pipeline. *Psychophysiology*, *57*(6), e13580. https://doi.org/10.1111/psyp.13580

Delorme, A., & Makeig, S. (2004). EEGLAB: An open source toolbox for analysis of single-trial EEG dynamics including independent component analysis. *Journal of Neuroscience Methods*, *134*(1), 9–21. https://doi.org/10.1016/j.jneumeth.2003.10.009

Demuru, M., & Fraschini, M. (2020). EEG fingerprinting: Subject-specific signature based on the aperiodic component of power spectrum. *Computers in Biology and Medicine*, *120*, 103748. https://doi.org/10.1016/j.compbiomed.2020.103748

Donoghue, T., Dominguez, J., & Voytek, B. (2020). Electrophysiological frequency band ratio measures conflate periodic and aperiodic neural activity. *ENeuro*, *7*(6), ENEURO.0192–ENEU20.2020. https://doi.org/10.1523/ENEURO.0192-20.2020

Donoghue, T., Haller, M., Peterson, E. J., Varma, P., Sebastian, P., Gao, R., Noto, T., Lara, A. H., Wallis, J. D., Knight, R. T., Shestyuk, A., & Voytek, B. (2020). Parameterizing neural power spectra into periodic and aperiodic components. *Nature Neuroscience*, *23*(12), 1655–1665. https://doi.org/10.1038/s41593-020-00744-x

Enders, C. K. (2013). Dealing with missing data in developmental research. *Child Development Perspectives*, *7*(1), 27–31. https://doi.org/10.1111/cdep.12008

Fló, A., Gennari, G., Benjamin, L., & Dehaene-Lambertz, G. (2022). Automated pipeline for infants continuous EEG (APICE): A flexible pipeline for developmental cognitive studies. *Developmental Cognitive Neuroscience*, *54*, 101077. https://doi.org/10.1016/j.dcn.2022.101077

Fransson, P., Metsäranta, M., Blennow, M., Åden, U., Lagercrantz, H., & Vanhatalo, S. (2013). Early development of spatial patterns of power-law frequency scaling in fMRI resting-state and EEG data in the newborn brain. *Cerebral Cortex*, *23*(3), 638–646. https://doi.org/10.1093/cercor/bhs047

Gabard-Durnam, L., & McLaughlin, K. A. (2020). Sensitive periods in human development: Charting a course for the future. *Current Opinion in Behavioral Sciences*, *36*, 120–128. https://doi.org/10.1016/j.cobeha.2020.09.003

Gabard-Durnam, L. J., Wilkinson, C., Kapur, K., Tager-Flusberg, H., Levin, A. R., & Nelson, C. A. (2019). Longitudinal EEG power in the first postnatal year differentiates autism outcomes. *Nature Communications*, *10*(1), 4188. https://doi.org/10.1038/s41467-019-12202-9

Gao, R., Peterson, E. J., & Voytek, B. (2017). Inferring synaptic excitation/inhibition balance from field potentials. *NeuroImage*, *158*, 70–78. https://doi.org/10.1016/j.neuroimage.2017.06.078

Gasser, T., Verleger, R., Bächer, P., & Sroka, L. (1988). Development of the EEG of school-age children and adolescents. I. Analysis of band power. *Electroencephalography and Clinical Neurophysiology*, *69*(2), 91–99. https://doi.org/10.1016/0013-4694(88)90204-0

Gilmore, J. H., Knickmeyer, R. C., & Gao, W. (2018). Imaging structural and functional brain development in early childhood. *Nature Reviews Neuroscience*, *19*(3), 123–137. https://doi.org/10.1038/nrn.2018.1

Graham, J. W. (2009). Missing data analysis: Making it work in the real world. *Annual Review of Psychology*, *60*(1), 549–576. https://doi.org/10.1146/annurev.psych.58.110405.085530

He, B. J. (2014). Scale-free brain activity: Past, present, and future. *Trends in Cognitive Sciences*, *18*(9), 480–487. https://doi.org/10.1016/j.tics.2014.04.003

Hill, A. T., Clark, G. M., Bigelow, F. J., Lum, J. A. G., & Enticott, P. G. (2022). Periodic and aperiodic neural activity displays age-dependent changes across early-to-middle childhood.

Developmental Cognitive Neuroscience, *54*, 101076. https://doi.org/10.1016/j.dcn.2022.101076

Immink, M. A., Cross, Z. R., Chatburn, A., Baumeister, J., Schlesewsky, M., & Bornkessel-Schlesewsky, I. (2021). Resting-state aperiodic neural dynamics predict individual differences in visuomotor performance and learning. *Human Movement Science*, *78*, 102829. https://doi.org/10.1016/j.humov.2021.102829

Jacob, M. S., Roach, B. J., Sargent, K. S., Mathalon, D. H., & Ford, J. M. (2021). Aperiodic measures of neural excitability are associated with anticorrelated hemodynamic networks at rest: A combined EEG-fMRI study. *NeuroImage*, *245*, 118705. https://doi.org/10.1016/j.neuroimage.2021.118705

John, A. M., Kao, K., Choksi, M., Liederman, J., Grieve, P. G., & Tarullo, A. R. (2016). Variation in infant EEG power across social and nonsocial contexts. *Journal of Experimental Child Psychology*, *152*, 106–122. https://doi.org/10.1016/j.jecp.2016.04.007

Karalunas, S. L., Ostlund, B. D., Alperin, B. R., Figuracion, M., Gustafsson, H. C., Deming, E. M., Foti, D., Antovich, D., Dude, J., Nigg, J., & Sullivan, E. (2022). Electroencephalogram aperiodic power spectral slope can be reliably measured and predicts ADHD risk in early development. *Developmental Psychobiology*, *64*(3), e22228. https://doi.org/10.1002/dev.22228

Leach, S. C., Morales, S., Bowers, M. E., Buzzell, G. A., Debnath, R., Beall, D., & Fox, N. A. (2020). Adjusting ADJUST: Optimizing the ADJUST algorithm for pediatric data using geodesic nets. *Psychophysiology*, *57*(8), e13566. https://doi.org/10.1111/psyp.13566

Liechti, M. D., Valko, L., Müller, U. C., Döhnert, M., Drechsler, R., Steinhausen, H. C., & Brandeis, D. (2013). Diagnostic value of resting electroencephalogram in attention-deficit/hyperactivity disorder across the lifespan. *Brain Topography*, *26*(1), 135–151. https://doi.org/10.1007/s10548-012-0258-6

MacNeill, L. A., Ram, N., Bell, M. A., Fox, N. A., & Pérez-Edgar, K. (2018). Trajectories of Infants' biobehavioral development: Timing and rate of A-not-B performance gains and EEG maturation. *Child Development*, *89*(3), 711–724. https://doi.org/10.1111/cdev.13022

Marshall, P. J., Bar-Haim, Y., & Fox, N. A. (2002). Development of the EEG from 5 months to 4 years of life. *Clinical Neurophysiology*, *113*(8), 1199–1208. https://doi.org/10.1016/S1388-2457(02)00163-3

Matta, T. H., Flournoy, J. C., & Byrne, M. L. (2018). Making an unknown unknown a known unknown: Missing data in longitudinal neuroimaging studies. *Developmental Cognitive Neuroscience*, *33*, 83–98. https://doi.org/10.1016/j.dcn.2017.10.001

McSweeney, M., Morales, S., Valadez, E. A., Buzzell, G. A., & Fox, N. A. (2021). Longitudinal age- and sex-related change in background aperiodic activity during early adolescence. *Developmental Cognitive Neuroscience*, *52*, 101035. https://doi.org/10.1016/j.dcn.2021.101035

Nakagawa, S., Johnson, P. C., & Schielzeth, H. (2017). The coefficient of determination R 2 and intra-class correlation coefficient from generalized linear mixed-effects models revisited and expanded. *Journal of the Royal Society Interface*, *14*(134), 20170213. https://doi.org/10.1098/rsif.2017.0213

Nolan, H., Whelan, R., & Reilly, R. B. (2010). FASTER: Fully automated statistical thresholding for EEG artifact rejection. *Journal of Neuroscience Methods*, *192*(1), 152–162. https://doi.org/10.1016/j.jneumeth.2010.07.015

Ogrim, G., Kropotov, J., & Hestad, K. (2012). The quantitative EEG theta/beta ratio in ADHD and normal controls: Sensitivity, specificity, and behavioral correlates. *Psychiatry Research*, *198*(3), 482–488. https://doi.org/10.1016/j.psychres.2011.12.041

Orekhova, E. (1999). Theta synchronization during sustained anticipatory attention in infants over the second half of the first year of life. *International Journal of Psychophysiology*, *32*(2), 151–172. https://doi.org/10.1016/s0167-8760(99)00011-2

Orekhova, E. V., Stroganova, T. A., & Posikera, I. N. (2001). Alpha activity as an index of cortical inhibition during sustained internally controlled attention in infants. *Clinical Neurophysiology*, *112*(5), 740–749. https://doi.org/10.1016/S1388-2457(01)00502-8

Orekhova, E. V., Stroganova, T. A., Posikera, I. N., & Elam, M. (2006). EEG theta rhythm in infants and preschool children. *Clinical Neurophysiology*, *117*(5), 1047–1062. https://doi.org/10.1016/j.clinph.2005.12.027

Ostlund, B., Donoghue, T., Anaya, B., Gunther, K. E., Karalunas, S. L., Voytek, B., & Pérez-Edgar, K. E. (2022). Spectral parameterization for studying neurodevelopment: How and why. *Developmental Cognitive Neuroscience*, *54*, 101073. https://doi.org/10.1016/j.dcn.2022.101073

Ostlund, B. D., Alperin, B. R., Drew, T., & Karalunas, S. L. (2021). Behavioral and cognitive correlates of the aperiodic (1/f-like) exponent of the EEG power spectrum in adolescents with and without ADHD. *Developmental Cognitive Neuroscience*, *48*, 100931.

Perone, S., Palanisamy, J., & Carlson, S. M. (2018). Age-related change in brain rhythms from early to middle childhood: Links to executive function. *Developmental Science*, *21*(6), e12691. https://doi.org/10.1111/desc.12691

Rayson, H., Debnath, R., Alavizadeh, S., Fox, N., Ferrari, P. F., & Bonaiuto, J. J. (2022). Detection and analysis of cortical beta bursts in developmental EEG data. *Developmental Cognitive Neuroscience*, *54*, 101069. https://doi.org/10.1016/j.dcn.2022.101069

Robertson, M. M., Furlong, S., Voytek, B., Donoghue, T., Boettiger, C. A., & Sheridan, M. A. (2019). EEG power spectral slope differs by ADHD status and stimulant medication exposure in early childhood. *Journal of Neurophysiology*, *122*(6), 2427–2437. https://doi.org/10.1152/jn.00388.2019

Saby, J. N., & Marshall, P. J. (2012). The utility of EEG band power analysis in the study of infancy and early childhood. *Developmental Neuropsychology*, *37*(3), 253–273. https://doi.org/10.1080/87565641.2011.614663

Samaha, J., & Cohen, M. X. (2022). Power spectrum slope confounds estimation of instantaneous oscillatory frequency. *NeuroImage*, *250*, 118929. https://doi.org/10.1016/j.neuroimage.2022

Schaworonkow, N., & Voytek, B. (2021). Longitudinal changes in aperiodic and periodic activity in electrophysiological recordings in the first seven months of life. *Developmental Cognitive Neuroscience*, *47*, 100895. https://doi.org/10.1016/j.dcn.2020.100895

Shuffrey, L. C., Pini, N., Potter, M., Springer, P., Lucchini, M., Rayport, Y., Sania, A., Firestein, M., Brink, L., Isler, J. R., Odendaal, H., & Fifer, W. P. (2022). Aperiodic electrophysiological activity in preterm infants is linked to subsequent autism risk. *Developmental Psychobiology*, *64*(4), e22271. https://doi.org/10.1002/dev.22271

Stroganova, T. A., Orekhova, E. V., & Posikera, I. N. (1999). EEG alpha rhythm in infants. *Clinical Neurophysiology*, *110*(6), 997–1012. https://doi.org/10.1016/S1388-2457(98)00009-1

Tierney, A. L., Gabard-Durnam, L., Vogel-Farley, V., Tager-Flusberg, H., & Nelson, C. A. (2012). Developmental trajectories of resting EEG power: An endophenotype of autism spectrum disorder. *PLoS One*, *7*(6), e39127. https://doi.org/10.1371/journal.pone.0039127

Trujillo, C. A., Gao, R., Negraes, P. D., Gu, J., Buchanan, J., Preissl, S., Wang, A., Wu, W., Haddad, G. G., Chaim, I. A., Domissy, A., Vandenberghe, M., Devor, A., Yeo, G. A., Voytek, B., & Muotri, A. R. (2019). Complex oscillatory waves emerging from cortical organoids model early human brain network development. *Cell Stem Cell*, *25*(4), 558–569. https://doi.org/10.1016/j.stem.2019.08.002

van Ede, F., Quinn, A. J., Woolrich, M. W., & Nobre, A. C. (2018). Neural oscillations: Sustained rhythms or transient burst-events? *Trends in Neurosciences*, *41*(7), 415–417. https://doi.org/10.1016/j.tins.2018.04.004

Voytek, B., & Knight, R. T. (2015). Dynamic network communication as a unifying neural basis for cognition, development, aging, and disease. *Biological Psychiatry*, *77*(12), 1089–1097. https://doi.org/10.1016/j.biopsych.2015.04.016

Voytek, B., Kramer, M. A., Case, J., Lepage, K. Q., Tempesta, Z. R., Knight, R. T., & Gazzaley, A. (2015). Age-related changes in 1/f neural electrophysiological noise. *Journal of Neuroscience*, *35*(38), 13257–13265. https://doi.org/10.1523/JNEUROSCI.2332-14.2015

Wang, J., Barstein, J., Ethridge, L. E., Mosconi, M. W., Takarae, Y., & Sweeney, J. A. (2013). Resting state EEG abnormalities in autism spectrum disorders. *Journal of Neurodevelopmental Disorders*, *5*(1), 1–14. https://doi.org/10.1186/1866-1955-5-24

West, B. T., Welch, K. B., & Galecki, A. T. (2006). *Linear mixed models: A practical guide using statistical software*. Chapman and Hall/CRC.

Whedon, M., Perry, N. B., & Bell, M. A. (2020). Relations between frontal EEG maturation and inhibitory control in preschool in the prediction of children's early academic skills. *Brain and Cognition*, *146*, 105636. https://doi.org/10.1016/j.bandc.2020.105636

Wilkinson, C., Pierce, L. J., Sideridis, G., Wade, M., & Nelson, C. A. (2023). Associations between EEG trajectories, family income, and cognitive abilities over the first two years of life. *Developmental Cognitive Neuroscience*, 101260. https://doi.org/10.1016/j.dcn.2023.101260

Xie, W., Mallin, B. M., & Richards, J. E. (2018). Development of infant sustained attention and its relation to EEG oscillations: An EEG and cortical source analysis study. *Developmental Science*, *21*(3), e12562. https://doi.org/10.1111/desc.12562

Yücel, M. A., Selb, J., Cooper, R. J., & Boas, D. A. (2014). Targeted principle component analysis: A new motion artifact correction approach for near-infrared spectroscopy. *Journal of Innovative Optical Health Sciences*, *7*(02), 1350066. https://doi.org/10.1142/S1793545813500661

SUPPORTING INFORMATION

Additional supporting information can be found online in the Supporting Information section at the end of this article.

TABLE S1. Demographic information of the sample that was included in the linear mixed models' analysis. The table presents the mean (SD) of the gestational weeks, gestational weight, and age of participants in each session.

TABLE S2. Demographic information of the included sample in the pairwise Spearman correlations between age sessions. Data: mean (SD).

TABLE S3. The goodness of the fit of the model (R^2 index) provided by the specparam toolbox for each session in different channel locations (clusters). All the infants included in the analysis had at least, a 0.95 value of fit.

TABLE S4. Descriptive statistics of the aperiodic parameters. Mean (SD) in each age and topographic location divided by sex.

TABLE S5. Descriptive statistics of the periodic power (microvolts) in each frequency band and cluster. Mean (SD).

TABLE S6. Descriptive statistics of the relative power (percentage) in each frequency band and cluster. Mean (SD).

TABLE S7. Model fit in each frequency range.

TABLE S8. Included participants in the linear mixed models for each epoch length and condition.

TABLE S9. Descriptives of the theta peak by cluster and session. It displays the percentage of channels with a peak (standard deviation) and the mean frequency (standard deviation) of the channels.

TABLE S10. Total sample (female) in the stability analysis per condition and epoch length.

FIGURE S1. Schematic representation of the pre-processing steps of the EEG signal.

FIGURE S2. The layout of the high-density net was employed in the study. The red color represents the removed electrodes in the first pre-processing step. The rest of the colors show the clusters: frontal (blue), central (pink), parietal (yellow), and occipital (green).

FIGURE S3. Aperiodic parameters (exponent and offset) development. The grey lines represent the individual trajectory while the red line represents the average trajectory.

FIGURE S4. Alpha peak frequency (top) and periodic power (bottom) development. In the upper figure, the grey lines represent the individual trajectory while the red line represents the average trajectory. In the bottom plot, the solid line represents the mean, and the shaded area is twice the standard error.

FIGURE S5. Relative power development for each frequency band and cluster. The grey lines represent individual trajectories and the red line the average trajectory.

FIGURE S6. Periodic power development for each frequency band and cluster. The grey lines represent individual trajectories and the red line the average trajectory.

FIGURE S7. Model Fit in all the frequency ranges employed in the computation of the aperiodic and periodic components.
FIGURE S8. Absolute (solid) and aperiodic (dotted) power for the 1 to 20 Hz and 1 to 45 Hz rangers and the 1 to 45 Hz range in each cluster. The plot displays the mean (solid line) and the standard error (shaded area) multiplied by 2.
FIGURE S9. Developmental changes in the aperiodic parameters per condition, frequency, and epoch length. The color represents the t-values of the Time fixed effect in the linear mixed models (red: positive, blue: negative).
FIGURE S10. Developmental changes in the relative and periodic power per condition, frequency band, and epoch length. The color represents the t-values of the Time fixed effect in the linear mixed models (red: positive, blue: negative).
FIGURE S11. Development of alpha peak frequency. The color represents the t-values of the Time fixed effect in the linear mixed models for each condition and epoch length.
FIGURE S12. Development of theta peak frequency. The color represents the t-values of the Time fixed effect in the linear mixed models for each condition and epoch length.
FIGURE S13. Stability of the aperiodic parameters in the combined condition in comparison to the conditions individually. The color represents Spearman's rho values (red: positive, blue: negative).
FIGURE S14. Stability of the power in the combined condition in comparison to the conditions individually. The color represents Spearman's rho values (red: positive, blue: negative).
FIGURE S15. Aperiodic parameters differences between the bubbles and video blocks. The color represents the *t*-values (blue: greater in bubbles).
FIGURE S16. Aperiodic parameters differences between the bubbles and video blocks. The color represents the *t*-values (red: greater in video, blue: greater in bubbles).
FIGURE S17. Correlation between the relative power and the aperiodic and periodic components for each frequency band and session age. The color represent the Spearman's rho values (red: positive, blue: negative).
FIGURE S18. Differences between the aperiodic and periodic contributions to the relative power. The colors represent the Fisher's *z* values and higher values mean larger correlation of the periodic power.

How to cite this article: Rico-Picó, J., Moyano, S., Conejero, Á., Hoyo, Á., Ballesteros-Duperón, M. Á., & Rueda, M. R. (2023). Early development of electrophysiological activity: Contribution of periodic and aperiodic components of the EEG signal. *Psychophysiology*, *00*, e14360. https://doi.org/10.1111/psyp.14360